IEEE Access
Multidisciplinary | Rapid Review | Open Access Journal

Received 22 October 2023, accepted 31 December 2023, date of publication 9 January 2024, date of current version 22 January 2024.

Digital Object Identifier 10.1109/ACCESS.2024.3351605

RESEARCH ARTICLE

Investigation of Patellar Deep Tendon Reflex Using Millimeter-Wave Radar and Motion Capture Technologies

DREW G. BRESNAHAN, (Member, IEEE), SCOTT KOZIOL, (Member, IEEE), AND YANG LI, (Senior Member, IEEE)
Department of Electrical and Computer Engineering, Baylor University, Waco, TX 76798, USA
Corresponding author: Drew G. Bresnahan (drew_bresnahan@alumni.baylor.edu)

This work was supported in part by the U.S. National Science Foundation under Grant 1609371.

This work involved human subjects or animals in its research. The authors confirm that all human/animal subject research procedures and protocols are exempt from review board approval.

ABSTRACT Physicians typically measure deep tendon reflexes visually, leading to ambiguity and disagreement over exact reflex classification. Millimeter-wave radar addresses this problem by providing an accurate, unambiguous measurement of reflex limb motion and features noncontact sensing for convenience and patient comfort. Radar spectrograms closely match optical motion capture results, supporting radar's viability as a clinical assessment tool. This study analyzes data from 60 radar and motion capture measurement trials across four subjects. Six reflex characteristics are defined and extracted. The extracted parameters show a high level of agreement between the two different techniques, with a mean relative error of only 10.39%. Additionally, a positive correlation was observed between hammer tap speed and reflex response speed, with maximum leg velocities showing a slope of 0.4. This study also quantifies and discusses the effects of hammer tap speed and leg length. An analytical model is derived to describe the patellar DTR system dynamics. In the future, physicians may use a specialized radar system to assess reflex performance quickly, accurately, and comfortably for a patient under test.

INDEX TERMS Human activity recognition, body sensor networks, biomedical applications of radiation, millimeter wave radar, clinical neuroscience.

I. INTRODUCTION

Deep tendon reflexes (DTR) are fundamental biomechanical responses that can help demonstrate general neurological health of a human patient [1]. Also known as a muscle stretch reflex, a DTR is an involuntary motor reaction caused by striking a tendon and stretching the nearby muscle tissue. Medical professionals use DTR tests to identify possible medical conditions like stroke, injury, neurodegenerative diseases, or damage from invasive surgery [2], [3]. To test for a reflex response, the clinician strikes the tendon of interest with a specialized reflex hammer [4] and visually observes the motor reaction.

Two well-established scales are currently used to quantify a reflex response, the NINDS (National Institute of Neurological Disorders and Stroke) myotatic reflex scale [5] (Table 1) and the Mayo Clinic scale [6]. Both scales provide an approximate description of reflex magnitudes such as "reflex in upper half of range," "brisk", or "low response."

While administering a DTR test is relatively simple and efficient, physicians may struggle to collect unambiguous quantitative information from DTRs by visual observation alone [2], leading to disagreement between doctors' diagnoses. This problem is intensified when attempting to discern small changes in one patient's reflex over time,

The associate editor coordinating the review of this manuscript and approving it for publication was Amjad Ali.

TABLE 1. NINDS myotatic reflex scale.

Score	Description
0	Reflex absent.
1	Reflex small, less than normal; includes a trace response or a response brought out only with reinforcement.
2	Reflex in lower half of normal range.
3	Reflex in upper half of normal range.
4	Reflex enhanced, more than normal; includes clonus if present, which optionally can be noted in an added verbal description of the reflex.

like when the patient is recovering from an injury involving nerve damage. A higher level of measurement detail would enable physicians to better evaluate DTR motion with extreme precision.

Many previous works have developed techniques to quantify the DTR response with precision unmatched by the human eye. Salazar-Muñoz et al. [7] constructed a controlled hammer-strike and leg swing detection system using an angular displacement accelerometer and gyroscope. After applying principal component analysis and running different combinations of data parameters through four data classifier models, the researchers found that a Naïve Bayes classifier could classify the data into the appropriate NINDS scale with 89.62% accuracy. Tham et al. [8] used motion capture (mocap) technology to evaluate the effect of increasing hammer tap velocity on patellar reflex reaction. Across 100 subjects (50 male and 50 female), the study showed a positive correlation between tendon tap velocity and leg swing angle. This study focused on the repeatability and reliability of mocap as a measurement tool and evaluated the coefficient of determination for the regression line modeling the relationship between tap speed and leg velocity to be 98.9%. Zhang et al. [9] created a reflex torque measurement system where the subject leg is linked to a mechanical force sensor while the hammer strike is applied. This researcher studied the custom-defined reflex parameters across tens of subjects and developed a model for classifying healthy and hemiplegic DTR performance. Other types of sensing techniques including EMG and ultrasound [10], [11], [12], [13] have also been used to measure DTRs. Table 2 summarizes a broad range of previous works and their main characteristics.

The above research works have mainly employed wearable sensors (accelerometer and gyroscope, mechanical force sensor, etc.) to quantify DTR responses, but little to no work has been conducted regarding noncontact reflex sensing. Short range, millimeter-wave radar is well-suited for noncontact, precise, and unambiguous DTR measurement. Millimeter-wave radar costs substantially less than motion capture systems, requires a fraction of the space, and features contactless sensing for minimum patient interaction and setup time. Radar has been successfully applied in many prior human motion studies such as gait analysis [14], [15], driver head motion detection [16], [17], and vital signs detection [18], [19], and is expected to perform well in capturing the micro-Doppler effects [20], [21], from limb motion caused by a DTR elicitation.

TABLE 2. Summary of previous DTR studies.

Reference Number	Sensor	Measured Quantities	Setup Complexity
[7]	Angular rate sensor	Angular velocity vs. time	Medium
[8]	Mocap	Knee angle, knee velocity	High
[9]	Torque sensor	Reflex impulse response	Medium
[10]	Accelerometer	Acceleration vs. time	Low
[11]	MMG and EMG	Voltage (EMG), displacement (MMG), frequency	Medium
[12]	Mocap	Max knee angle	High
[13]	Ultrasound	Muscle fiber velocities	Medium

Our previous study demonstrated the first use of radar to capture human patellar and triceps DTR motion [22]. However, the previous measurement was limited to a single test subject and one hammer striking speed. The focus of this work is to expand the scope of our study to use both a millimeter-wave radar and an optical motion capture system to simultaneously measure and characterize DTR responses for varying experiment variables such as hammer tap speeds, multiple subjects, left and right legs, and different leg lengths. This pilot study provides evidence for the accuracy and reliability of radar as a non-contact method for measuring human DTRs. With further validation in larger-scale studies, radar may serve as a standalone measurement tool without the need for additional motion capture systems. The technical objectives of this work are threefold: 1) to introduce and validate millimeter-wave radar as a noncontact method to measure human DTR motion, 2) to visualize the time-varying features of the DTR response by generating spectrogram images from radar data, and 3) to quantify the relationship between reflex hammer tap speed and various reflex parameters.

II. DATA COLLECTION METHODOLOGY

This study was conducted using the Texas Instruments® AWR1642BOOST [23] and DCA1000EVM [24] assembly. The 3.6 GHz bandwidth of this mm-wave FMCW radar facilitates a 4.17 cm range resolution. A shorter chirp period allows for a higher maximum measurable velocity, which is set at 7.33 m/s in this case. The frame period controls the slow time sampling rate (50 fps), which is sufficiently high for capturing a DTR response. Four human subjects were measured for this study; their physical information is tabulated in Table 3. Human testing was approved by the Baylor University IRB, protocol number IRB00002777. Informed consent was received from all human test subjects.

TABLE 3. Test subject physical information.

	Age (years)	Sex	Weight (kg)	Height (cm)	Leg Length (cm)
Subject 1	27	Male	80	188	96
Subject 2	24	Male	74	185	90
Subject 3	26	Male	93	165	80
Subject 4	25	Female	46	153	77

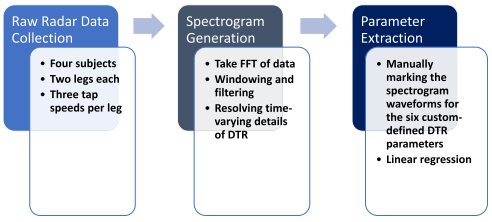

FIGURE 1. Data collection and processing pipeline.

A flowchart of the data collection and processing pipeline is shown in Fig. 1. Sections II and III explain this process in detail.

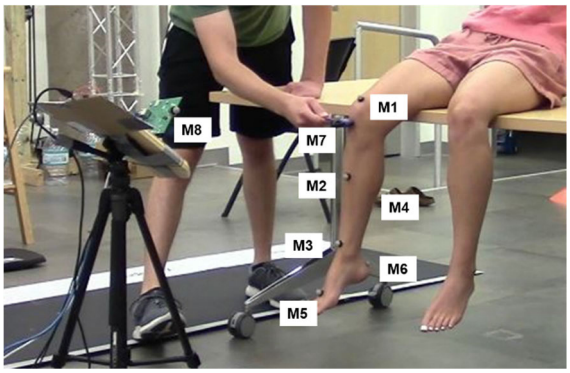

FIGURE 2. Experiment setup showing placement of test subject, radar, and reflex hammer user for the patellar reflex. The subject is seated on a wooden table with mocap markers on her leg.

Fig. 2 shows the measurement setup for recording the patellar reflex motion. The radar assembly is positioned on a tripod and is pointed 45° below the horizontal with respect to the ground to aim at the test subject's leg. The subject is seated on a wooden table one meter away from the radar with his or her legs allowed to swing freely.

A Vicon Nexus® [25] passive motion capture system is used in tandem with the radar to provide an alternative way to record DTR. The radar and motion capture system are triggered simultaneously to capture DTR data at a rate of 50 frames per second. Six motion capture markers are placed on the subject's leg: on the kneecap (M1), shin (M2), ankle (M3), middle-back of leg (M4), top of toes (M5), and back of heel (M6). One marker is placed on the reflex hammer to capture the hammer tap speed (M7), and a reference marker is placed on the stationary radar (M8). Fig. 2 shows the marker placement for the patellar reflex measurement.

An Arduino®microcontroller is used to simultaneously trigger the radar and mocap system at the press of a button. After triggering the start command, a researcher uses a reflex hammer to strike the subject's patellar tendon. The limb reacts with the characteristic forward jerk of the deep tendon reflex, and the limb is allowed to swing back and forth naturally until it comes to a rest. This procedure is repeated for multiple cycles during the recording to ensure a consistent, repeatable response is recorded. Nine trials are conducted for each test subject. The reflex hammer tap speed is varied across the nine trials, approximately "slow" (1.5–2 m/s), "medium" (2–3 m/s), and "fast" (3–4 m/s). Three trials of each speed are collected for each subject. The hammer tap is not mechanically controlled, resulting in a spread of different tap speeds.

The radar data is post-processed using custom MATLAB®
code. Each radar frame is processed using the two-dimensional fast Fourier transform, which resolves the downrange distance and velocity information. Then, each frame is compressed into a single range bin and concatenated in chronological order to create the spectrogram of target velocity versus time. We characterize the DTR using velocity relative to the radar since it is similar to the perspective of a clinician eliciting and observing a DTR. The acceleration or distance information could be acquired by taking the derivative or integral of velocity, respectively.

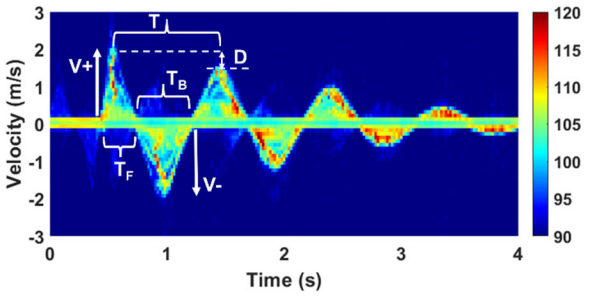

FIGURE 3. Spectrogram of a single patellar DTR trial showing velocity across time with parameter annotations.

III. PARAMETER EXTRACTION RESULTS

Fig. 3 shows a radar-measured sample spectrogram of a single DTR response (subject 1, left leg, medium hammer speed). The vertical axis corresponds to velocity with respect to the radar (positive values represent forward movement and negative values represent backward movement), and the color represents the radar return signal strength on a relative decibel scale. The DTR response starts around 0.5 seconds, where the leg begins to swing toward the radar. The leg achieves its first positive velocity peak at 0.65 seconds, and it gradually decays to zero at 0.88 seconds where the leg stops at its swinging peak. Then the leg begins to swing backward, away from the radar, finishing its first backward swing at 1.3 seconds. Such forward-backward swing cycles repeat as time goes

on, but with decaying reflex magnitude. The DTR response diminishes to zero around 4 seconds.

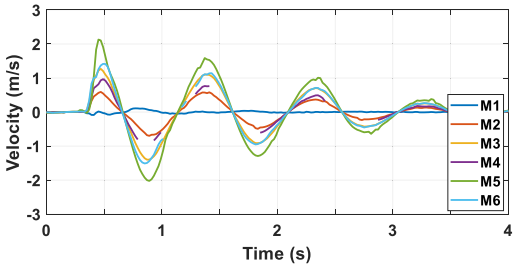

FIGURE 4. Motion capture of a single patellar DTR trial showing velocity across time for each leg marker.

Fig. 4 plots the mocap-measured velocity vs. time series for each of the six markers used in the same trial as that of Fig. 3. The velocities are all calculated relative to the stationary radar marker (M8) to directly correlate with the radar's velocity measurements. Clearly, the marker with the best fit to the radar spectrogram envelope is M5, which is placed in the lowest position on the leg and generates the largest velocity component. All other markers move more slowly due to the pendulum-like nature of the swinging leg. By visual inspection, there is a clear agreement between the radar and mocap results.

In this study, we extract the following six parameters from both radar and mocap measurement data to succinctly quantify the DTR response: maximum positive velocity (V+), maximum negative velocity (V-), duration of the first forward swing (T_F), duration of the first backward swing (T_B), period between first and second peak (T), and damping factor between first and second peak (D). These parameters have been annotated in Fig. 3. In total, 60 DTR experimental trials are conducted (3 subjects * 2 legs * 9 hammer speeds, plus 1 subject * 2 legs * 3 hammer speeds), resulting in 360 data points (6 parameters of interest * 60 trials).

As an example, the extracted maximum positive velocity (V+) values from radar and mocap measurements are plotted in Figs. 5(a) and (b), respectively. The two plots are very similar to each other. Each plot has 60 data points, with four different colors representing four subjects and two different shapes representing two legs (circle for right leg and square for left leg). To analyze the data, we used linear regression to model the correlation between the DTR parameter magnitudes (velocity, period, duration, damping) and the hammer tap speed. The linear regression analysis produced two lines for each DTR parameter, one for the right leg data (solid black) and one for the left leg data (dashed black) across all subjects, respectively, indicating a significant positive correlation between hammer tap speed and the magnitude of the DTR parameter. It is apparent that the maximum positive velocity of the DTR increases as the hammer tap velocity increases. Although not shown here, similar observations can be made for the maximum negative velocity (V-).

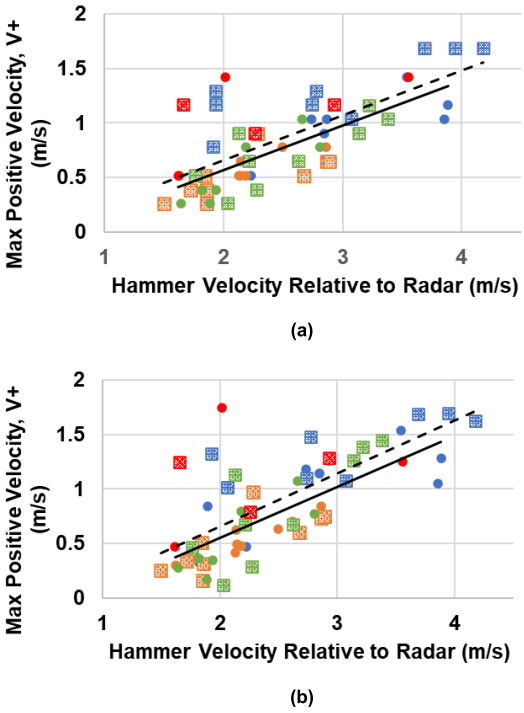

FIGURE 5. Scatter plots showing max positive velocity (V+) vs. hammer tap speed: (a) radar and (b) mocap. Each color is a unique test subject. Circles are right leg and squares are left leg. Right leg regression line is solid and left leg regression line is dashed.

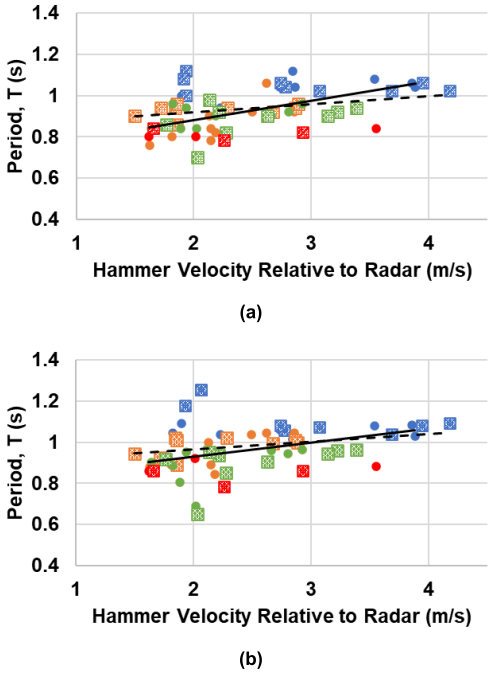

FIGURE 6. Scatter plots showing period (T) vs. hammer tap speed: (a) radar and (b) mocap. Each color is a unique test subject. Circles are right leg and squares are left leg. Right leg regression line is solid and left leg regression line is dashed.

The extracted period (T) values from radar and mocap measurements are plotted in Figs. 6(a) and (b), respectively. The

data series shape, color, and regression line representations are the same as in Fig. 5. Figs. 6(a) and (b) are very similar to each other, showing good agreement between radar and mocap. The regression line slopes in Fig. 6 are much less steep compared to those of the V+ values in Fig. 5, indicating the period is less sensitive to a changing hammer tap speed. Although not shown here, similar observations can be made for the duration of the first forward swing (T_F) and duration of the first backward swing (T_B).

To quantify the difference between the radar and motion capture results, the average absolute relative error for each DTR parameter is computed using equation (1) below. N (=60) represents the number of data points in each scatterer plot, and $r(i)$ and $m(i)$ represent corresponding individual extracted values for each point in the radar and mocap scatter plots, respectively.

$$Rel.Error = \frac{1}{N}\sum_{i=1}^{N}\left|\frac{r(i)-m(i)}{r(i)}\right| \times 100\% \qquad (1)$$

The average relative error results for all six DTR parameters are displayed in Table 4. The backward duration (T_B) and period (T) have the smallest relative error, while max positive velocity (V+) and damping factor (D) have the greatest. The differences are explained as consequences of limited radar velocity resolution compared to the extreme precision of motion capture cameras. Nevertheless, there is no relative error that exceeds 15%, which supports the viability of the radar as a clinical DTR measurement device.

TABLE 4. Average relative error per DTR parameter.

	V+	V-	T_F	T_B	T	D
Average Relative Error (%)	13.98	10.35	13.03	4.47	5.70	14.83

IV. DISCUSSIONS

The measurement results collected above can provide insights on the patellar DTR response and its relationship with the test subjects and the striking hammer. Between Figs. 5 and 6, three common observations are made: (1) the V+ plots have a much steeper slope than the T plots, (2) the slower hammer speeds appear to have a wider vertical spread of data than the faster speeds, and (3) the test subjects appear to occupy separate regions of the scatter charts, albeit substantial overlap. These observations are discussed in detail next.

A. DTR SENSITIVITY DUE TO TAP SPEED

Previous works have documented a relationship between hammer tap speed and DTR response parameters. Tham et al. [8] presented a chart showing maximum leg angular velocity versus hammer drop release angle. They found a distinctly linear relationship between the two variables. Zhang et al. [26] also found a correlation between hammer tap speed and reflex torque through linear regression.

In our analysis, we also investigate the sensitivity of the DTR parameters due to tap speed of the striking hammer. The maximum positive velocity (V+) is substantially correlated with the hammer striking speed, as shown by the steep slope of the regression lines in Fig. 5. In contrast, the period (T) is much less sensitive to varying hammer striking speeds, as shown by the relatively flat slope of the regression lines in Fig. 6. Therefore, the slopes of the regression lines provide a good indication of how sensitive each DTR responses with respect to changing tap speed.

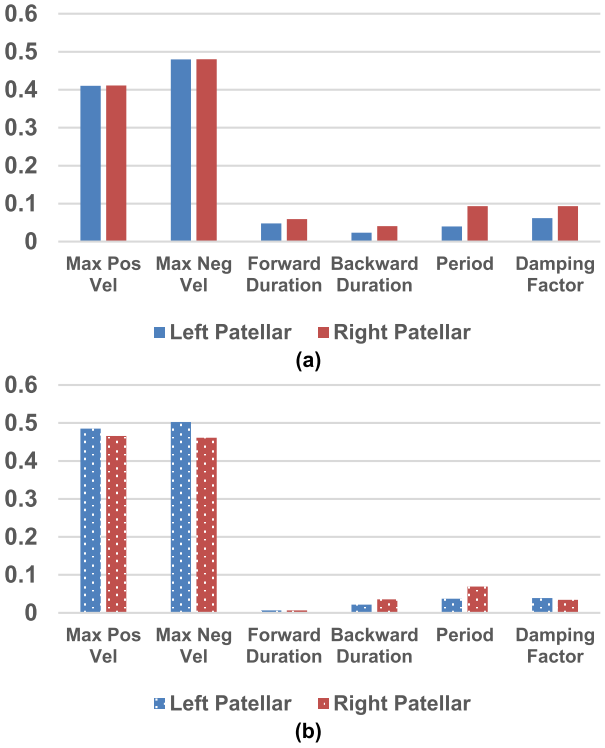

FIGURE 7. Bar chart showing the slopes of respective regression lines of all parameters for the left and right patellar reflex as measured by the (a) radar and (b) Vicon® motion capture system.

We extract the regression line slopes from the radar results for all six parameters, as shown in Fig. 7 (a) for both left and right patellar data. The max positive and max negative velocities (V+, V-) clearly exhibit the greatest sensitivity to tap speed, while the other parameters show very little sensitivity to tap speed. The mocap data shown in Fig. 7 (b) are similar and confirm the findings. Furthermore, the left and right patellar reflexes are reasonably balanced across all parameters, as indicated by the similar slopes. This is expected since none of the test subjects suffer from peripheral neuropathy that would cause an imbalance in reflex laterality such as nerve damage or lesions in the reflex arc.

B. DATA SPREAD DUE TO TAP SPEED

To ensure a properly stimulated DTR response, the hammer speed must be above a certain threshold value. At the same time, clinicians cannot strike the patient too hard lest they cause pain or damage to the limb in question.

Archambeault et al. [27] showed that there is a nonlinear, sigmoid-shaped function approximating the tendon EMG response amplitude versus hammer impact velocity with R^2 of 96%. Similar phenomena were documented by [28]. Hammer strikes that are too weak or too strong will not help clinicians classify DTRs, but the approximately linear region in the middle is the most helpful model for building a reliable, consistent reflex stimulus profile.

By quantifying the spread of the data relative to the total linear regression line (including left and right leg data), we can find the tap speed region that best creates a consistent and predictable DTR response with the least variation from the regression line. From the visual inspection of the Figs. 5 and 6 in section III, we surmised that the data caused by slower tap speeds, approximately 2.5 m/s or less, were more spread out from the regression line than the data caused by faster tap speeds. By separately calculating the coefficient of determination (R^2) for the two segments of the data, we can compare the spread of data before and after 2.5 m/s tap speed on the horizontal axis. R^2 is given as

$$R^2 = 1 - \frac{RSS}{TSS} \tag{2}$$

where *RSS* is the sum of squares of the residuals, and *TSS* is the sum of squares of each data point relative to the mean. "Residual" is defined as the difference between the data point and the regression line. This comparison is shown in the bar chart in Fig. 8(a) for the radar data and Fig. 8(b) for the mocap data.

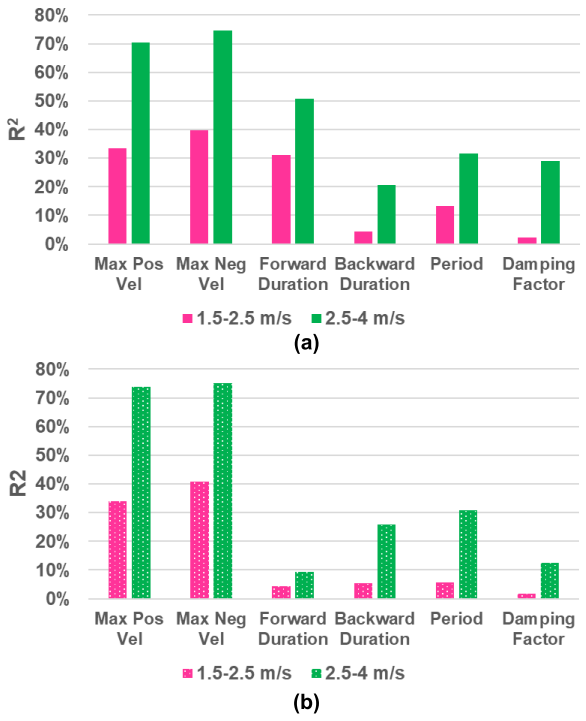

FIGURE 8. R^2 values for two sections of the (a) radar and (b) mocap dataset: those data with less than 2.5 m/s tapping speed, and those data with greater than 2.5 m/s tapping speed.

In both figures, the data from the higher tap speeds (green) is substantially more fit to the total regression line than the data from lower tap speeds (pink), as indicated by the higher R^2 values. This finding leads credence to the notion that clinicians administering a DTR test must strike the tendon with a firm, moderately fast tap as opposed to a soft, slow tap. The highest R^2 values belong to the max positive and max negative velocity parameters, indicating that the total regression lines for those scatter plots do the best job of modeling the variation in their respective data. The timing parameters do not achieve similarly high R^2 values since their variation is not modeled as well by their flatter regression lines. However, the comparison between slower and faster tap speeds for all parameters shows a consistent message: tap speeds above 2.5 m/s generate reflex responses that are less varied and more consistent with respect to the total regression line.

C. DTR TIMING PARAMETERS AFFECTED BY LEG LENGTH

Finally, we consider the effect of leg length on the various measured parameters for patellar reflexes. By taking the average value of the DTR parameters across hammer tap speeds in the 2.5–3 m/s region and plotting versus the leg length of each subject, we can better understand the effect leg length has on these parameters. The decision to only average the data from tap speeds of 2.5–3 m/s is to remove the variability due to slower tap speeds, and to conform the tap speeds to a similar range for all subjects.

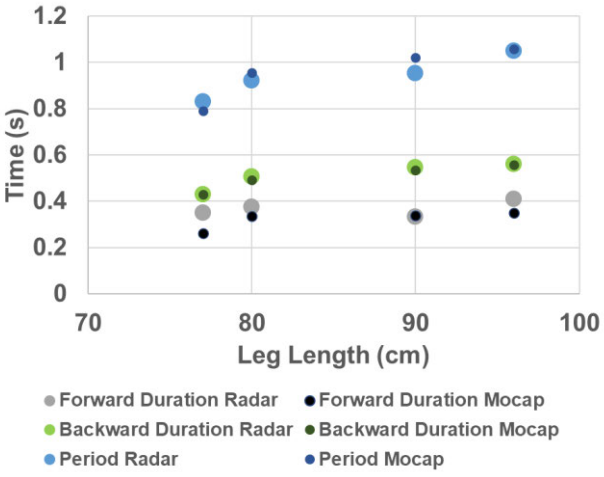

FIGURE 9. Time parameters vs leg length across four test subjects.

This analysis was applied to all six reflex parameters, but only the three timing parameters (TF, TB, T) produced a positive correlation result. Fig. 9 shows the leg length study for radar data and mocap data. There is a slight positive slope present for each series, indicating there is indeed some correlation between longer legs and longer duration of timing parameters of DTRs. This should be expected, assuming a leg swings with the oscillation mechanics of a swinging pendulum.

V. PARAMETER IDENTIFICATION USING DYNAMIC SYSTEM MODELING

In addition to employing mm-wave radar and motion capture measurement techniques, it is possible to generate and analyze the DTR response from a systems modeling and systems identification perspective [30]. These theoretical predictions not only serve to corroborate the measurement findings but also offer deeper insights into the physical relationships governing how various physiological parameters (such as leg length, leg mass, mass moment of inertia, etc.) influence the DTR responses.

Previous work has attempted to model the knee as a damped pendulum [31] and [33]. In those works, the authors modeled the leg's swinging motion using differential equations. We also model the motion using differential equations; however, we express the dynamic motion as an impulse response. Specifically, a linear differential equation can be used to model the dynamic motion of a swinging leg, and then the leg's dynamic motion can be analytically studied using an impulse response [30].

TABLE 5. Impulse response model parameter estimates for subject 4.

Parameters	Description	Value
m	Mass of leg below knee	4.2 kg [31]
L	Distance estimate between the knee and the ankle	0.385 m
J	Mass moment of inertia	0.2075 [31]
g	Gravity	9.8 m/s^2
B	Viscous Friction Coefficient	0.15 Nms/rad

We have derived a model estimate of the leg's angular velocity impulse response, $\tilde{h}_{\substack{\text{leg angular}\\ \text{velocity}}}(t)$, as depicted in equation (3). A comprehensive account of the derivation, though extensive, will be presented in an upcoming publication. Furthermore, in Table 4, we provide a list of model parameters along with their representative values estimated for Subject 4. Parameters such as mass (m), length (L), and moment of inertia (J) can be estimated based on the leg's physical characteristics. Notably, the friction parameter (B) [32] plays a significant role in influencing the damping of oscillations and is empirically determined through curve fitting to experimental data.

$$\tilde{h}_{\substack{\text{leg angular}\\ \text{velocity}}}(t) = \underbrace{\left[\frac{1}{xJ}e^{-\frac{B}{2J}t}\right]}_{\text{damping term}}\underbrace{\left[x\cos(xt) - \frac{B}{2J}\sin(xt)\right]}_{\text{oscillating term}} \tag{3}$$

where:

$$x = \left(mg\frac{L}{J2} - \frac{B^2}{4J^2}\right)^{\frac{1}{2}} \tag{4}$$

To facilitate a comparison with our mocap and spectrogram data, we must convert the angular velocity derived from Eq. (3) into a linear velocity estimate. To illustrate, we estimate the linear velocity of the extended toes, as described in equation (5), by multiplying the angular velocity from Eq. (3) by the distance from the knee to the outstretched toes, denoted as "d_{toe}."

$$\tilde{v}_{toe}(t) = d_{toe}\tilde{h}_{\substack{\text{leg angular}\\ \text{velocity}}}(t) \tag{5}$$

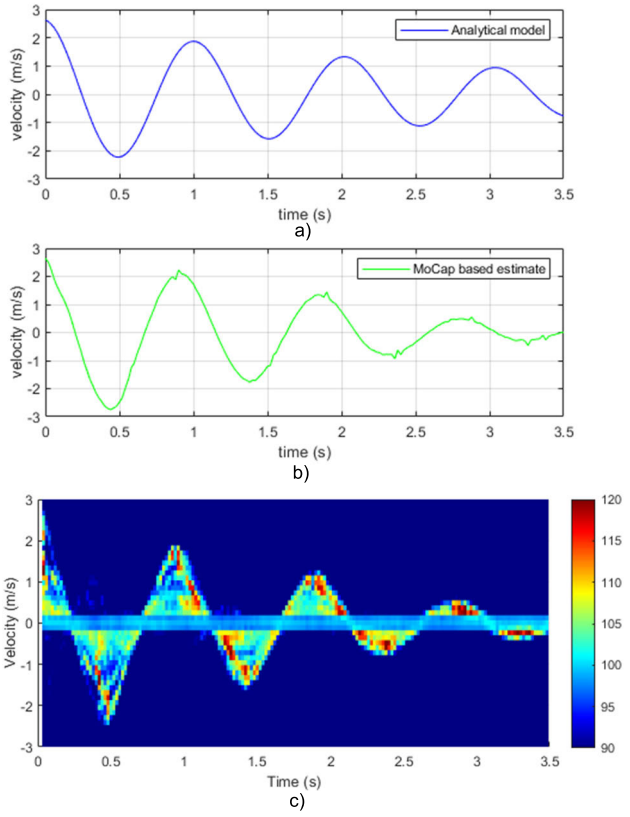

FIGURE 10. Validating the derived impulse response equation and model parameters (Table 5) by comparing it to Mocap and spectrogram data from subject 4. a) The response from the analytically derived impulse response prediction of a DTR (where model constants B=0.15, m = 4.2, L =0.385, g = 9.8, dtoe = 0.584); b) Linear velocity estimate of the toe based on Mocap data; c) spectrogram data.

Figure 10 presents a comparison of the predicted toe velocity (a) for a single DTR trial with the estimated toe velocity derived from motion capture measurements (b) and mm-wave radar (c). The plotted data represent the envelope of the spectrogram, specifically the outermost contour tracing the damped oscillations resulting from the motion of the fastest moving part, namely the tips of the toes. The striking similarity in terms of both velocity and timing parameters observed in these graphs instills confidence in the accuracy of our impulse response model, as described in equation (3), especially when coupled with the model parameters fitted and outlined in Table 5. This alignment between the model predictions and the actual measurements affirms the reliability of our approach in estimating the impulse response of a DTR response.

VI. CONCLUSION AND FUTURE WORK

This study focused on the use of radar to measure patellar muscle stretch reflexes, the comparison of radar results to motion capture results, and analysis of the collected data and its trends. Using radar and mocap, we measured the patellar DTR response of four subjects for 60 trials, extracting six custom DTR parameters. The average relative error between radar and mocap is less than 15%. We discussed three characteristics observed from the DTR responses: (i) the velocity parameters are substantially more sensitive to hammer tap speed than the timing parameters; (ii) the slower tap speeds (< 2.5 m/s) produce less predictable responses than faster tap speeds; and (iii) longer leg lengths cause a measurable increase in the duration and period of the DTR leg motion.

The primary limitations of this work are the small number of available test subjects, the radar's required position in front of the test subject, and the lack of a controlled reflex hammer delivery system. However, these limitations can be addressed in future work by expanding the pool of test subjects and implementing a dedicated hammer control system. Future studies could also consider including test subjects with hyperreflexia or hyporeflexia and an imbalance in reflex laterality to further explore the potential clinical capabilities of mm-wave radar to diagnose or monitor patients. The dataset from this study is publicly available at IEEE DataPort [29].

From these studies, radar has proven to be a reliable measurement technology that has great potential to quantify patellar reflexes in clinical settings. Patellar reflexes are not the only DTRs that radar can measure. Future studies should analyze the triceps reflex and extend radar's reach as a medical assessment tool. Future studies should also consider test subjects with hyperreflexia or hyporeflexia with an imbalance in reflex laterality to further explore radar's utility in clinical settings for patients with different ailments.

ACKNOWLEDGMENT

The authors would like to thank the test subjects for their contribution to this work.

REFERENCES

[1] H. K. Walker, "Deep tendon reflexes," in *Clinical Methods: The History, Physical, and Laboratory Examinations*, 3rd ed. Boston, MA, USA: Butterworths, 1990, ch. 72, pp. 123–135. [Online]. Available: https://www.ncbi.nlm.nih.gov/books/NBK396/

[2] G. L. Marshall and J. W. Little, "Deep tendon reflexes: A study of quantitative methods," *J. Spinal Cord Med.*, vol. 25, no. 2, pp. 94–99, Jul. 2002, doi: 10.1080/10790268.2002.11753608.

[3] J. P. R. Dick, "The deep tendon and the abdominal reflexes," *J. Neurol., Neurosurg. Psychiatry*, vol. 74, no. 2, pp. 150–153, Feb. 2003, doi: 10.1136/jnnp.74.2.150.

[4] O. Lin-Wei, L. L. S. Xian, V. T. W. Shen, C. Y. Chuan, S. A. Halim, A. R. I. Ghani, Z. Idris, and J. M. Abdullah, "Deep tendon reflex: The tools and techniques. What surgical neurology residents should know," *Malaysian J. Med. Sci.*, vol. 28, no. 2, pp. 48–62, Apr. 2021, doi: 10.21315/mjms2021.28.2.5.

[5] M. Hallett, "NINDS myotatic reflex scale," *Neurology*, vol. 43, no. 12, p. 2723, Dec. 1993, doi: 10.1212/wnl.43.12.2723.

[6] Mayo Clinic Staff, *Mayo Clinic Examinations in Neurology*, 7th ed. Maryland Heights, MI, USA: Mosby, 1998.

[7] Y. Salazar-Muñoz, B. E. García-Caballero, R. Muñoz-Ríos, G. A. López-Pérez, and L. A. Ruano-Calderon, "Angular rate measurement in the assessment of patellar reflex," in *Proc. 13th Int. Conf. Power Electron. (CIEP)*, Jun. 2016, pp. 192–197, doi: 10.1109/CIEP.2016.7530755.

[8] L. K. Tham, N. A. A. Osman, W. A. B. W. Abas, and K. S. Lim, "The validity and reliability of motion analysis in patellar tendon reflex assessment," *PLoS ONE*, vol. 8, no. 2, Feb. 2013, Art. no. e55702, doi: 10.1371/journal.pone.0055702.

[9] L.-Q. Zhang, G. Wang, J. Sliwa, and W. Z. Rymer, "Dynamics of patellar tendon reflex in spastic multiple sclerosis patients," in *Proc. 20th Annu. Int. Conf. IEEE Eng. Med. Biol. Soc.*, Nov. 1998, pp. 2313–2316, doi: 10.1109/IEMBS.1998.744751.

[10] R. Lemoyne, W. Kerr, K. Zanjani, and T. Mastroianni, "Implementation of an iPod wireless accelerometer application using machine learning to classify disparity of hemiplegic and healthy patellar tendon reflex pair," *J. Med. Imag. Health Informat.*, vol. 4, no. 1, pp. 21–28, Mar. 2014, doi: 10.1166/jmihi.2014.1219.

[11] H. Tsuji, H. Misawa, T. Takigawa, T. Tetsunaga, K. Yamane, Y. Oda, and T. Ozaki, "Quantification of patellar tendon reflex using portable mechanomyography and electromyography devices," *Sci. Rep.*, vol. 11, no. 1, Jan. 2021, Art. no. 2284, doi: 10.1038/s41598-021-81874-5.

[12] A. Chandrasekhar, N. A. A. Osman, L. K. Tham, K. S. Lim, and W. A. B. W. Abas, "Influence of age on patellar tendon reflex response," *PLoS ONE*, vol. 8, no. 11, Nov. 2013, Art. no. e80799, doi: 10.1371/journal.pone.0080799.

[13] S. Sikdar, M. Lebiedowska, A. Eranki, L. Garmirian, and D. Damiano, "Measurement of rectus femoris muscle velocities during patellar tendon jerk using vector tissue Doppler imaging," in *Proc. Annu. Int. Conf. IEEE Eng. Med. Biol. Soc.*, Sep. 2009, pp. 2963–2966, doi: 10.1109/IEMBS.2009.5332500.

[14] A.-K. Seifert, M. Grimmer, and A. M. Zoubir, "Doppler radar for the extraction of biomechanical parameters in gait analysis," *IEEE J. Biomed. Health Informat.*, vol. 25, no. 2, pp. 547–558, Feb. 2021, doi: 10.1109/JBHI.2020.2994471.

[15] Z. Chen, G. Li, F. Fioranelli, and H. Griffiths, "Personnel recognition and gait classification based on multistatic micro-Doppler signatures using deep convolutional neural networks," *IEEE Geosci. Remote Sens. Lett.*, vol. 15, no. 5, pp. 669–673, May 2018, doi: 10.1109/LGRS.2018.2806940.

[16] D. G. Bresnahan and Y. Li, "Classification of driver head motions using a mm-wave FMCW radar and deep convolutional neural network," *IEEE Access*, vol. 9, pp. 100472–100479, 2021, doi: 10.1109/ACCESS.2021.3096465.

[17] J. Jung, S. Lim, B.-K. Kim, and S. Lee, "CNN-based driver monitoring using millimeter-wave radar sensor," *IEEE Sensors Lett.*, vol. 5, no. 3, pp. 1–4, Mar. 2021, doi: 10.1109/LSENS.2021.3063086.

[18] A. Ahmad, J. C. Roh, D. Wang, and A. Dubey, "Vital signs monitoring of multiple people using a FMCW millimeter-wave sensor," in *Proc. IEEE Radar Conf.*, Apr. 2018, pp. 1450–1455, doi: 10.1109/RADAR.2018.8378778.

[19] J.-M. Muñoz-Ferreras, Z. Peng, R. Gómez-García, and C. Li, "Random body movement mitigation for FMCW-radar-based vital-sign monitoring," in *Proc. IEEE Topical Conf. Biomed. Wireless Technol., Netw., Sens. Syst. (BioWireleSS)*, Austin, TX, USA, Jan. 2016, pp. 22–24, doi: 10.1109/BIOWIRELESS.2016.7445551.

[20] V. C. Chen, *The Micro-Doppler Effect in Radar*, 2nd ed. Norwood, MA, USA: Artech House, 2019.

[21] S. S. Ram, C. Christianson, Y. Kim, and H. Ling, "Simulation and analysis of human micro-Dopplers in through-wall environments," *IEEE Trans. Geosci. Remote Sens.*, vol. 48, no. 4, pp. 2015–2023, Apr. 2010, doi: 10.1109/TGRS.2009.2037219.

[22] D. G. Bresnahan, G. Lee, and Y. Li, "Measurement of deep tendon reflexes using a millimeter-wave radar," *IEEE Sensors Lett.*, vol. 6, no. 5, pp. 1–4, May 2022.

[23] *AWR1642BOOST*. Accessed: Feb. 24, 2022. [Online]. Available: https://www.ti.com/tool/AWR1642BOOST

[24] *DCA1000EVM*. Accessed: Feb. 24, 2022. [Online]. Available: https://www.ti.com/tool/DCA1000EVM

[25] *Vicon Nexus*. Accessed: Feb. 24, 2022. [Online]. Available: https://www.vicon.com/software/nexus/

[26] L.-Q. Zhang, H. Huang, J. A. Sliwa, and W. Z. Rymer, "System identification of tendon reflex dynamics," *IEEE Trans. Rehabil. Eng.*, vol. 7, no. 2, pp. 193–203, Jun. 1999, doi: 10.1109/86.769410.
[27] M. Archambeault, H. de Bruin, A. McComas, and W. Fu, "Tendon reflexes elicited using a computer controlled linear motor tendon hammer," in *Proc. Int. Conf. IEEE Eng. Med. Biol. Soc.*, Aug. 2006, pp. 5068–5071, doi: 10.1109/IEMBS.2006.259923.
[28] J. Stam and H. van Crevel, "Measurement of tendon reflexes by surface electromyography in normal subjects," *J. Neurol.*, vol. 236, no. 4, pp. 231–237, May 1989, doi: 10.1007/BF00314505.
[29] D. G. Bresnahan, *Deep Tendon Reflex Measurement Data* (Radar and Motion Capture). Piscataway, NJ, USA: IEEE, Mar. 18, 2023, doi: 10.21227/9vbp-n597.
[30] G. F. Franklin, J. D. Powell, and A. Emami-Naeini, *Feedback Control of Dynamic Systems*, 2019.
[31] L. Vodovnik, B. R. Bowman, and T. Bajd, "Dynamics of spastic knee joint," *Med. Biol. Eng. Comput.*, vol. 22, no. 1, pp. 63–69, Jan. 1984.
[32] E. T. Enikov and G. Campa, "Mechatronic aeropendulum: Demonstration of linear and nonlinear feedback control principles with MATLAB/Simulink real-time windows target," *IEEE Trans. Educ.*, vol. 55, no. 4, pp. 538–545, Nov. 2012.
[33] T. Bajd and B. Bowman, "Testing and modelling of spasticity," *J. Biomed. Eng.*, vol. 4, no. 2, pp. 90–96, Apr. 1982.

DREW G. BRESNAHAN (Member, IEEE) was born in Plano, TX, USA, in 1994. He received the B.S., M.S., and Ph.D. degrees in electrical and computer engineering from Baylor University, in 2016, 2018, and 2022, respectively.

He has been with Raytheon Technologies Corporation, Dallas, TX, USA, since 2014, as a Hardware Test Engineer and a MMIC Design Engineer. His research interests include electromagnetic propagation, machine learning, and analysis of human body interactions with radar.

SCOTT KOZIOL (Member, IEEE) received the B.S. degree in electrical engineering from Cedarville University, Cedarville, OH, USA, in 1998, the M.S. degree in electrical engineering from Iowa State University, Ames, IA, USA, in 2000, and the M.S. degree in mechanical engineering and the Ph.D. degree in robotics from the Georgia Institute of Technology, Atlanta, GA, USA, in 2011 and 2013, respectively. He is currently an Associate Professor and the Associate Chair of the Department of Electrical and Computer Engineering, Baylor University, Waco, TX, USA.

YANG LI (Senior Member, IEEE) received the B.S. degree in electrical engineering from the University of Science and Technology of China, in 2005, and the M.S. and Ph.D. degrees in electrical and computer engineering from The University of Texas at Austin, in 2007 and 2011, respectively.

He joined Baylor University, in 2011, as a Faculty Member, where he is currently an Associate Professor in electrical and computer engineering. His research interests include body area electromagnetic wave propagation and antenna radiation, wearable antenna analysis and design, effective medium theory and homogenization technique, and micro-Doppler radar. He has authored 37 journal articles and 67 conference papers and abstracts. He serves as the General-Co Chair for the 2022 IEEE Texas Symposium on Wireless and Microwave Circuits and Systems.